DOI: 10.13009/EUCASS2023-091
Aerospace Europe Conference 2023 – 10TH EUCASS – 9TH CEAS

Mechanical design of a deployable morphing aeroshell for 12U CubeSat atmospheric re-entry

I. Dimino†, C. Vendittozzi§, W. R. Silva§, R. C. F. Mendez§, S. Ameduri*, L. Paglia# and F. Marra#*
**Adaptive Structures Division, CIRA, The Italian Aerospace Research Centre*
Via Maiorise 81043 Capua, Italy
i.dimino@cira.it*; s.ameduri@cira.it
§Campus FGA, Universidade de Brasília
St. Leste Projeção A - Gama Leste, Brasília - DF, 72444-240, Brasil
vendittozzi@unb.br; reis.william@unb.br
#Department of Chemical Engineering, Materials, Environment, Sapienza University of Rome,
INSTM Reference Laboratory for Engineering of Surface Treatments via Eudossiana 18, Rome, 00184, Italy
laura.paglia@uniroma1.it; francesco.marra@uniroma1.it
† Corresponding Author

Abstract

There is a wide application spectrum of deployable aeroshells for de-orbit and re-entry of space vehicles by using flexible heat shields. By expanding to a larger diameter prior to entry in order to increase drag, such a technology has shown to provide higher entry performance suitable for Earth or a variety of planetary high-speed entries that require high temperature thermal protection systems materials. Also, innovative shape-changing mechanisms exist in the literature for controlled re-entry and safe recovery of CubeSat class systems to recover payloads and data from LEO at low cost for post flight inspections and experimentations. Shape morphing during atmospheric entry could enable trajectory control by providing enhanced flight manoeuvrability and high-precision landing. This paper presents a CubeSat design concept that incorporates a mechanically deployable re-entry aeroshell within the standard 12U form factor by investigating aerodynamics and heating of a flexible thermal protection system having shape-changing capabilities. Focus is given to the design of the deployment system through structural simulations. The deployable surface can be modulated by a single actuator in order to modulate the lift-to-drag ratio for guided entry. Additionally, once deployed, the system can activate eight small movable aerodynamic flaps that can be individually morphed via a SMA-based actuation to control the trajectory and target the entry vehicle into the desired area for landing. This paper is framed within a joint research project for scientific and technological cooperation between Italy and Brazil in the field of space science, co-funded by the Italian Ministry of Foreign Affairs and International Cooperation (MAECI) and by CONFAP through the involved Brazilian State Funding Agencies (FAPs).

1. Introduction

A mechanically deployed system has the capability of deploying a load-bearing flexible thermal protection system (TPS) for high-speed atmospheric re-entry with a reduced ballistic coefficient [1]-[3]. In [4], the NASA ADEPT entry concept for standard CubeSat units has proven to deliver the same science payload with a stowed diameter 3-4 times smaller than an equivalent rigid aeroshell. The design uses an umbrella-like deployable structure with a 3-D woven carbon fabric to achieve more efficient packing and adequate thermal protection during entry. Similarly, a deployable Mars aeroshell concept is developed by O'Driscoll at alii [5].
Morphing technology can provide mechanically deployable aeroshells with improved entry conditions and landing precision suitable for safe and timely recovery of payloads and samples with reduced risks and costs [6]. Their ability to modulate the drag profile during re-entry operations offers considerable benefits over traditional rigid aeroshells that enable more accurate guidance trajectories and improved landing accuracy. Additionally, lower peak decelerations, heat loads and fluxes can be effectively achieved to protect the payload from the re-entry environment. Prior work on drag modulation have proven to guide a satellite to a desired re-entry interface point [7]. In [8], aerodynamic drag modulation of umbrella-like heat shield has shown to be an efficient way to control the re-entry location. An adaptive

DOI: 10.13009/EUCASS2023-091

aerobrake using aerodynamic flaps is also addressed in [9] to efficiently steer the vehicle during re-entry. In [10], such a technology is also combined with a fiber optics-based closed-loop feedback monitoring system in order to realize a full autonomous re-entry system. In [11]-[12], NASA's Pterodactyl project has focused on a deployable atmospheric entry vehicle (DEV) integrated with eight flaps mounted at the edge of the heatshield that can deflect in and out of the flow in order to provide precision targeting during re-entry. In [13], a preliminary conceptual analysis of a novel shape-changing concept using a SMA-based actuation is proposed for the control of morphing flaps separately.

This paper is framed within the context of the first executive programme for scientific and technological cooperation between Italy and Brazil supporting joint research projects for the years 2022-2024. A research on innovative mechanically deployable shape-changing re-entry aeroshells is carried out within the SPLASH (Self-DePloyable FLexible AeroSHell for de-Orbiting and Space Re-entry) project, funded by the Italian Ministry of Foreign Affairs and International Cooperation (MAECI) for the Italian side, and by National Council of State Research Support Foundations (CONFAP) through the involved Distrito federal Funding Agency (FAPDF) for the Brazilian side.

This paper describes the structural design activities carried out by the joint research team, coordinated by CIRA, for the development of such novel re-entry concept featuring advanced mechanism, flexible heat shield and smart actuation. The deployment mechanism is sized for a standard 12U CubeSat deployer, as shown in Figure 1, in order to take advantage of existing CubeSat deployment systems.

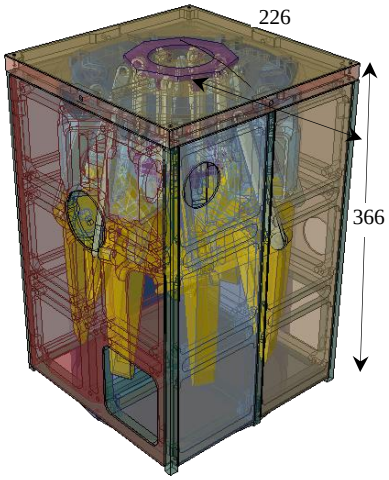

Figure 1: Preliminary SPLASH concept for 12U CubeSat Platform

2. Vehicle description

This paper deals with the preliminary design of a deployable atmospheric entry vehicle integrated with a morphing technology to provide additional precision targeting during re-entry of scientific missions in Low Earth Orbit (LEO). The system incorporates an innovative shape-changing mechanism that can be housed in the folded configuration inside a 12U Cubesat and then deployed with the intent of a re-entry and landing for payload recovery. The adaptive thermal protection system is a deployable umbrella-like heat shield consisting of structural ribs and struts, shown in Figure 2, that can be stowed at launch and deployed during re-entry to reduce the ballistic coefficient. This leads to reduced heat fluxes, mechanical loads and final descent velocity.

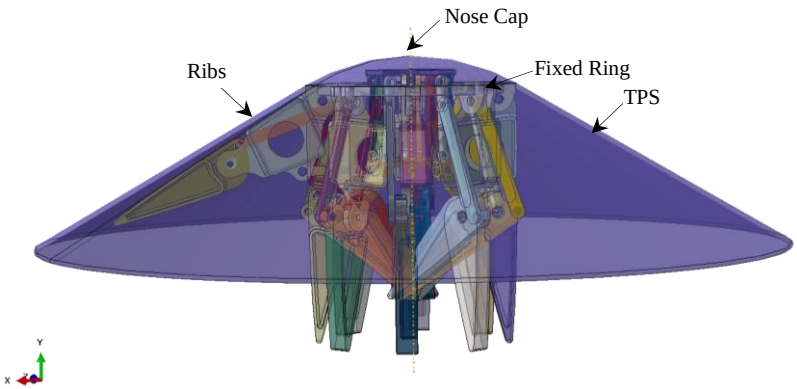

Figure 2: A general description of the aeroshell components

DOI: 10.13009/EUCASS2023-091

The structural skeleton consists of four primary components: nose cap, main body, ribs and struts [13]. The nose cap is designed to withstand aerothermal loads at the stagnation point. The thermal protection system includes also a flexible high temperature material for the conical part with heat and flame protection capability. When the TPS is completely deployed the base diameter is about 1 meter, while the cylindrical structure has a diameter of 21.6 cm. The structural skeleton consists of a multi-hinge assembly based on a set of finger-like articulations having two-modal capabilities:

- the deployable surface can be modulated by changing the sphere-cone angle, in order to provide drag modulation capabilities, control the trajectory and target the payload into the desired area for landing and recovery;
- Once deployed, the system can also activate eight small movable aerodynamic flaps that can be individually "morphed" to guarantee additional precision in landing and enhance the capsule maneuverability during the re-entry trajectory by using exclusively aerodynamic forces.

A moveable ring enables symmetrical rotation of the morphing ribs during deployment, as shown in Figure 3. It is connected to the morphing ribs though eight actuation rods that drive the rotation of the main hinges of the ribs during system deployment/retraction. The whole mechanism is controlled by a screw-jack actuator.
The morphing ribs incorporate two consecutive blocks connected by hinges so that the actuation leverages force the mechanism to rotate according to specific gear ratio depending on the position of the linking beams connecting the outer blocks to the fixed ring.

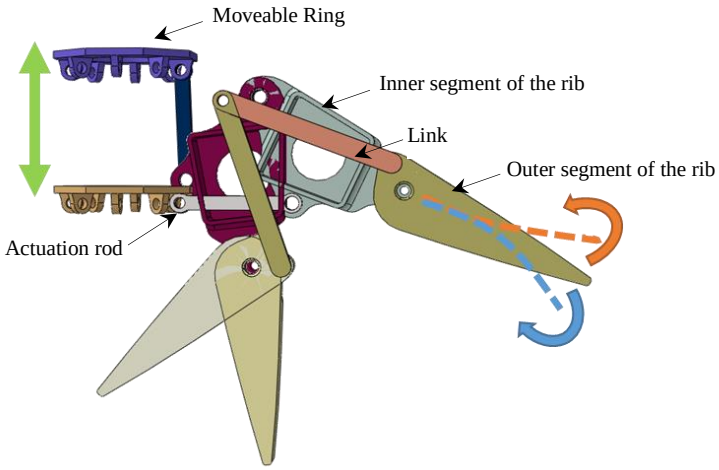

Figure 3. The deployment/retraction mechanism of a single rib with morphing capabilities [13]

Finally, when the deployable mechanism is locked in a given position, the outer segments of the ribs can be morphed by a shape memory alloy-based bending mechanism as active morphing flaps.

2.1 System configuration

As a very first approximation, a Newtonian approach is considered to estimate the spacecraft drag coefficient (CD) by simplifying its shape with a cone, as shown in Figure 4, by using the equation:

$$C_D = (1 - \sin^4 \delta_C)\left(\frac{r_n}{r_c}\right)^2 + 2\sin^2 \delta_C \left[1 - \left(\frac{r_n}{r_c}\right)^2 \cos^2 \delta_C\right] \quad \textbf{(1)}$$

where δ_C is the cone half angle, r_c is the cone base radius and r_n is the nose radius. A is the area of the frontal cross section, which is perpendicular to the motion direction.

DOI: 10.13009/EUCASS2023-091

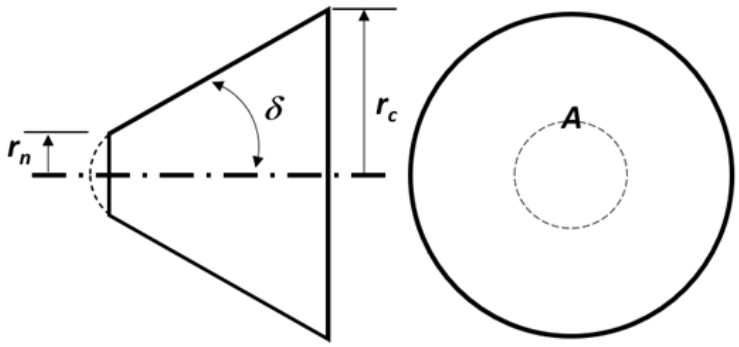

Figure 4: SPLASH concept configurations.

A nominal undeflected “rigid” surface is preliminary considered to compute drag and ballistic coefficients for various cone half angles, as shown in Table 1. We can calculate also the ballistic coefficient (BC) for a target mass of 24 kg of the spacecraft.

Table 1: Drag Coefficient (CD) and Ballistic Coefficient (BC)

r_n (m)	0.108	0.108	0.108	0.108
r_c (m)	0.305	0.35878	0.419	0.488
m (kg)	24	24	24	24
A (m^2)	0.2923	0.40439	0.551	0.749
δ_C (deg)	15	30	45	60
C_D	0.243	0.551	1.017	1.503
BC (kg/m^2)	337.779	107.716	42.882	21.306

3. Re-entry mission from LEO

The flight design scenario for the assessment of aerodynamics and aerothermodynamics of the SPLASH concept is shown in Figure 5. Table 2 shows examples of Earth entry environments from LEO that can be found in the literature for similar deployable vehicles [9], [14].

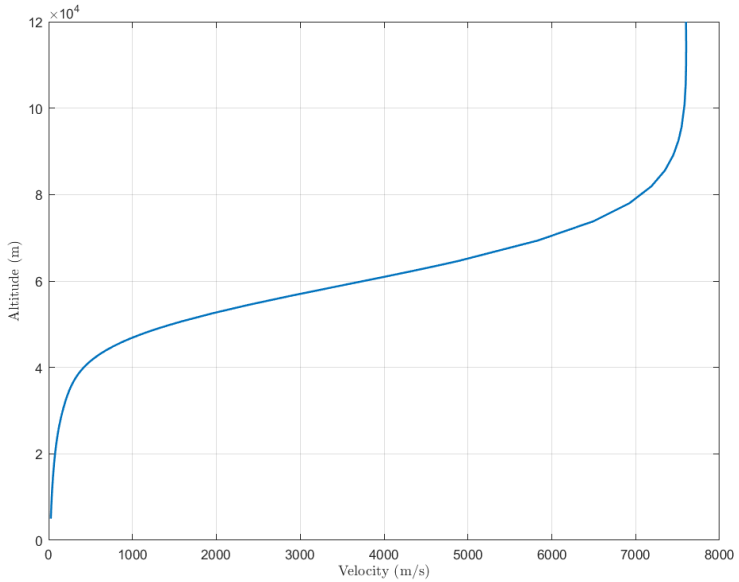

Figure 5. Altitude evolution vs. velocity. Re-entry from LEO.

DOI: 10.13009/EUCASS2023-091

Table 2: Earth Entry environments from LEO: Mini-IRENE [9], NanoADEPT [14], SPLASH capsules

	Earth Entry from LEO		
	Mini-IRENE [9]	Nano-ADEPT[14]	SPLASH
Velocity [m/s]	7600	7600	7600
Flight path angle [°]	-1	-1	-1
Sphere-cone angle [°]	45	70	60
Altitude [km]	120	120	120
Deployed diameter [m]	1.51	0.7	0.976
Entry mass [kg]	40	15	24
Ballistic coefficient [kg/m2]	21.28	22.5	21.34
Peak Heat flux [kW/m^2]	450	750	750

Figure 6 shows the stagnation point heat flux as a function of the altitude by considering a constant C_D. Comparison of the time history of the stagnation point heat flux between the SPLASH concept and Mini-IRENE [9] and Nano-ADEPT [14] capsules is shown in Figure 7 for a re-entry mission from LEO. The latter refer to the case of m= 40 kg and m= 15 kg, respectively, both having a similar ballistic coefficient. Fig. 8 shows the profile of dynamic pressure during the descent flight for the case of a constant C_D.

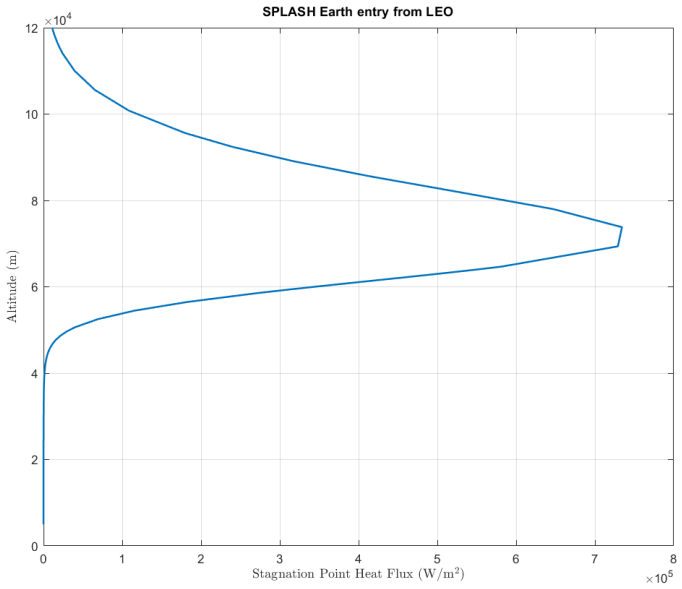

Figure 6. Stagnation point heat flux versus altitude in case of re-entry from LEO.

DOI: 10.13009/EUCASS2023-091

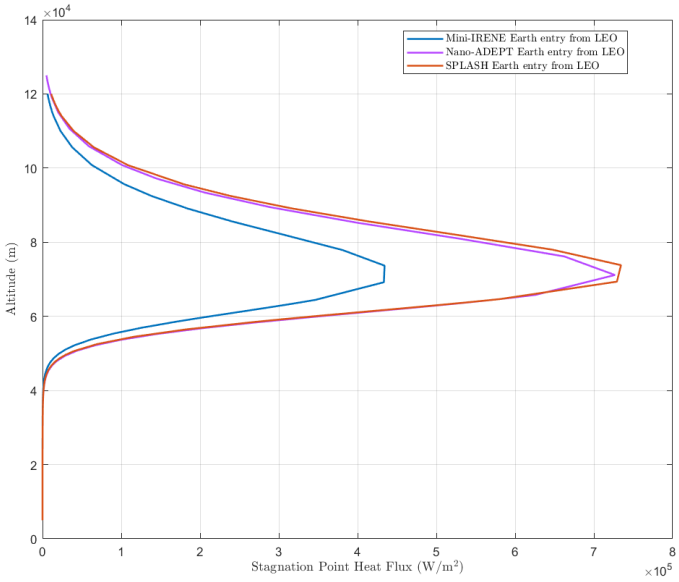

Figure 7. Comparison of stagnation point heat flux of SPLASH, MINI-IRENE [9] and Nano-ADEPT [14] concepts for a re-entry mission from LEO.

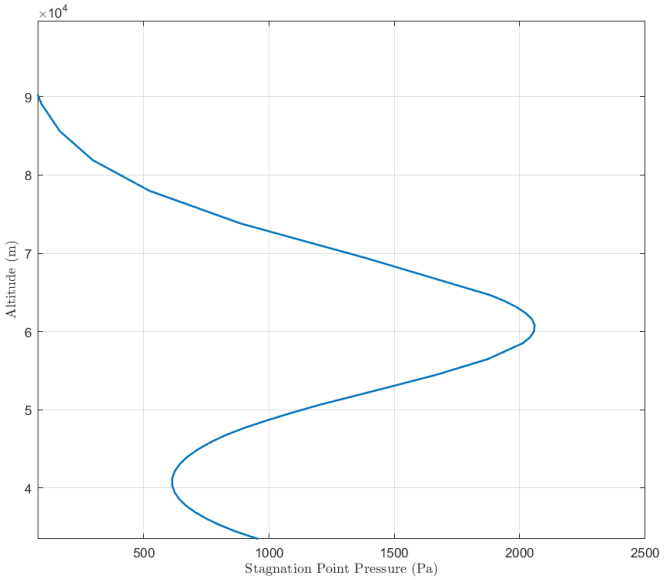

Figure 8. Stagnation point pressure for a re-entry mission from LEO.

It is worth noting that the highest value of pressure is experienced by the capsule at an altitude of about 60 km, whereas the peak of heat flux occurs at around 70 km. All the aerothermal analyses are carried out by using the HyperSMS Aerothermodynamic Tool [15]. Such a MATLAB® toolbox is quite reliable for the preliminary design of a re-entry non winged vehicle, keeping in consideration the different aspects involved in an atmospheric re-entry.
Such preliminary assessments of the aerothermal loading environment during the entire trajectory guide the preliminary design of the flexible heat shield by providing the pressure and heat flux distributions occurring on the capsule. The aeroheating environment dictates the type and size of the thermal protection system (TPS) while the choice of the thermal protection material typically depends on the peak heat rate. The integrated heat load dictates the thickness and hence the mass of the heat shield. Finally, pressure and shear stress acting on the heat shield determine the mechanical loads the capsule has to withstand during descent.

DOI: 10.13009/EUCASS2023-091

4. FE model of the deployed configuration

The flexible TPS of the capsule is one of the most critical parts of the SPLASH vehicle. Several tests were carried out at the Plasma Wind Tunnel test of CIRA to investigate thermal performance of Nextel material in past IRENE activities [16]. In this paper, starting from the rigid multi-body model detailed in [13], a modelling task was carried out by developing a specific approach aimed at describing the process of installation of the shield fabric, the consequent tensioning effect and the related impact of the external aerodynamic load. The tensioning process was addressed by fixing the fabric on the inner central circular border and stretching the eight outer vertices up to overlapping them to the tips of rigid beams replicating the inner structure. Then the vertices were linked to the tips to simulate the typical glove engagement and released to allow the achievement of the equilibrium between the fabric and the arms below. A uniform pressure of 2 kPa was then applied on the pretensioned shield. On this configuration, in the next steps of the research, the impact of the deflection of the arm tips will be estimated, considering the effect of the SMA actuators. After that, a finite element model of the capsule was developed to investigate both the stress distribution and the displacement field due to a preload acting on the TPS membrane when it was connected to the deployment mechanism.

4.1 Preload and symmetric pressure on the flexible TPS

The tensioning process of the flexible TPS was firstly investigated by using the non-linear sol 400 MSC/Nastran solver. This tool in fact allows the simulation of the large displacements imposed to the vertices of the shield, the change of the constraint condition due to the connection of the vertices to the arm tips and the displacement of the pre-tensioned shield membrane subjected to the external aerodynamic pressure. Moreover, the tool is also equipped with a dedicated card, MATSMA, implementing the SMA constitutive law. The process described above is illustrated in the block diagram shown in Figure 9.

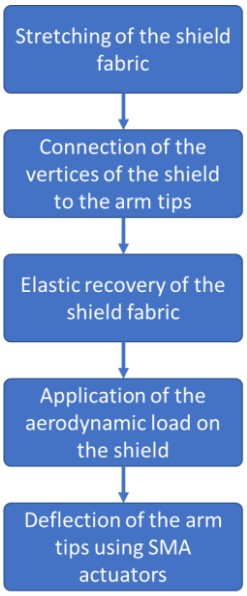

Figure 9. Modelling approach adopted to simulate the shield fabric integration and the action of the external aerodynamic load.

The simulation process was finalised within a unique subcase split into 3 steps. The first one was dedicated to the stretching; this operation was addressed using the SPCD cards applied at the 8 vertices of the shield moved towards the three directions to fill the current gap with the corresponding arm tips. The initial position of the vertices was defined by means of a scaling process applied on the entire shield and producing and initial truncated-cone shaped shield with the same frustum angle of the final stretched one and with a reduced height and diameter. The schemes of Figure 10 illustrate the type of transformation produced in the 1st step of the simulation and compare the initial and the final shield configurations. The FE model of the flexible TPS connected to the eight rigid beams representative of the deployment mechanism is shown in Figure 11.

DOI: 10.13009/EUCASS2023-091

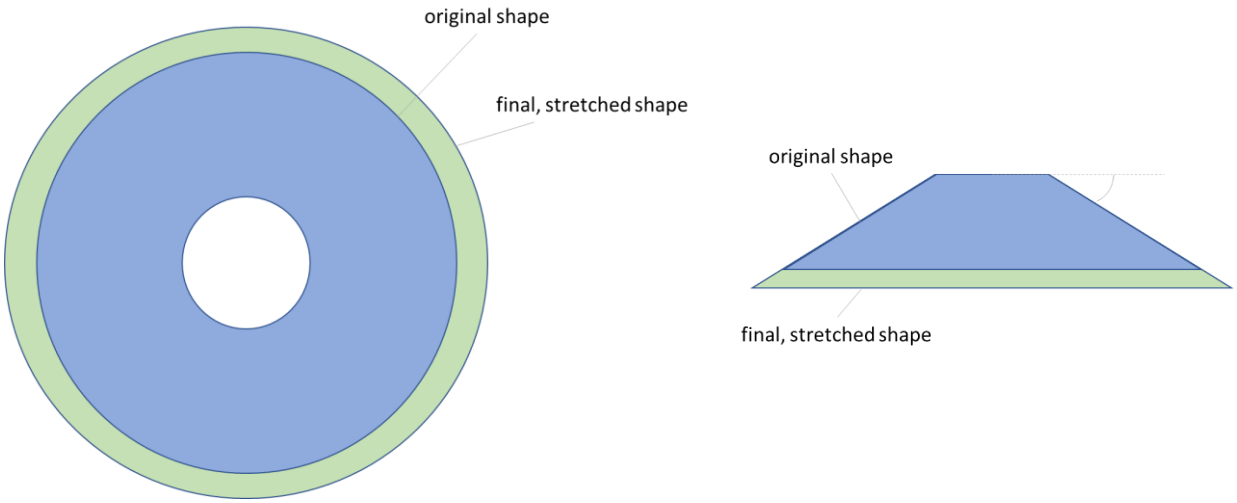

Figure 10. Initial truncated-cone shaped shield and final stretched one: top (a) and lateral (b) view.

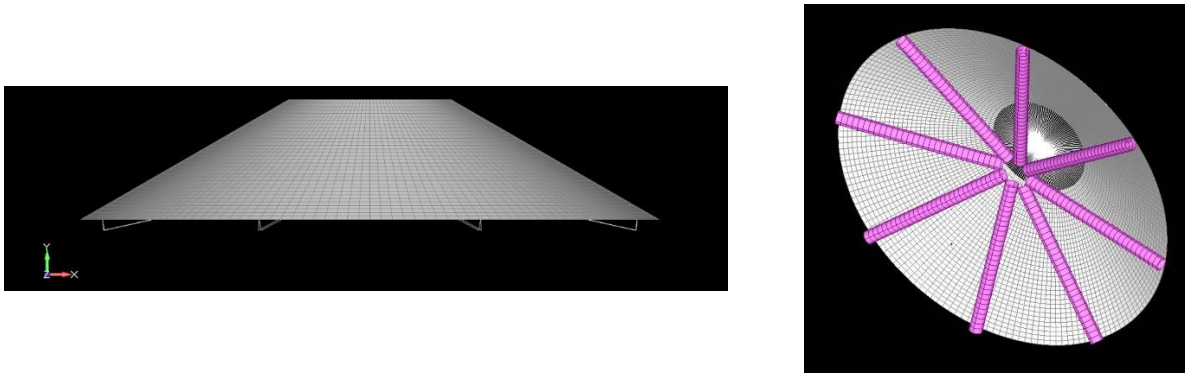

Figure 11. Lateral and bottom view of the FE model

At the beginning of the 2nd step, MPC cards are used to link the translational dofs of the vertices to the arm tips. After this operation, the elastic recovery of the shield occurs; this is possible for the absence in this step of the SPCD cards. This process continues as the equilibrium between the fabric and the arms is finally reached. Then the step 3 starts. The external aerodynamic pressure is applied normally to the shield that acts as a membrane stiffened by the tensional stress produced in the previous step. The configurations in terms of displacement and stress of the shield during the simulation are illustrated in Figure 12 (lateral view) and in Figure 13 (top view). Axial symmetry is observed.

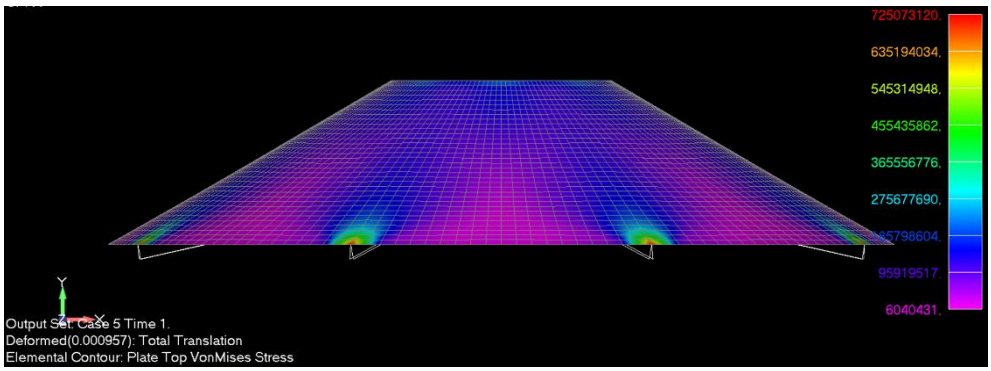

Fully stretched shield (end step 1)

DOI: 10.13009/EUCASS2023-091

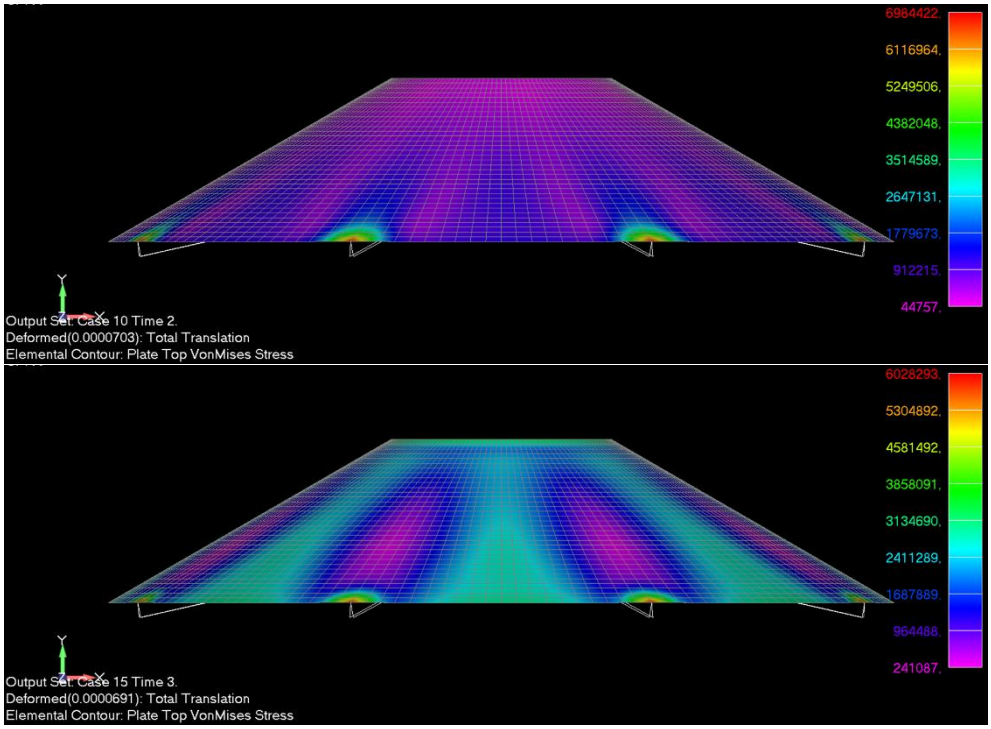

Linked and recovered shield (end of step 2)

Shield under the action of the external loads (end of step 3)

Figure 12. Displacement and stress on the shield during the simulation steps, lateral view.

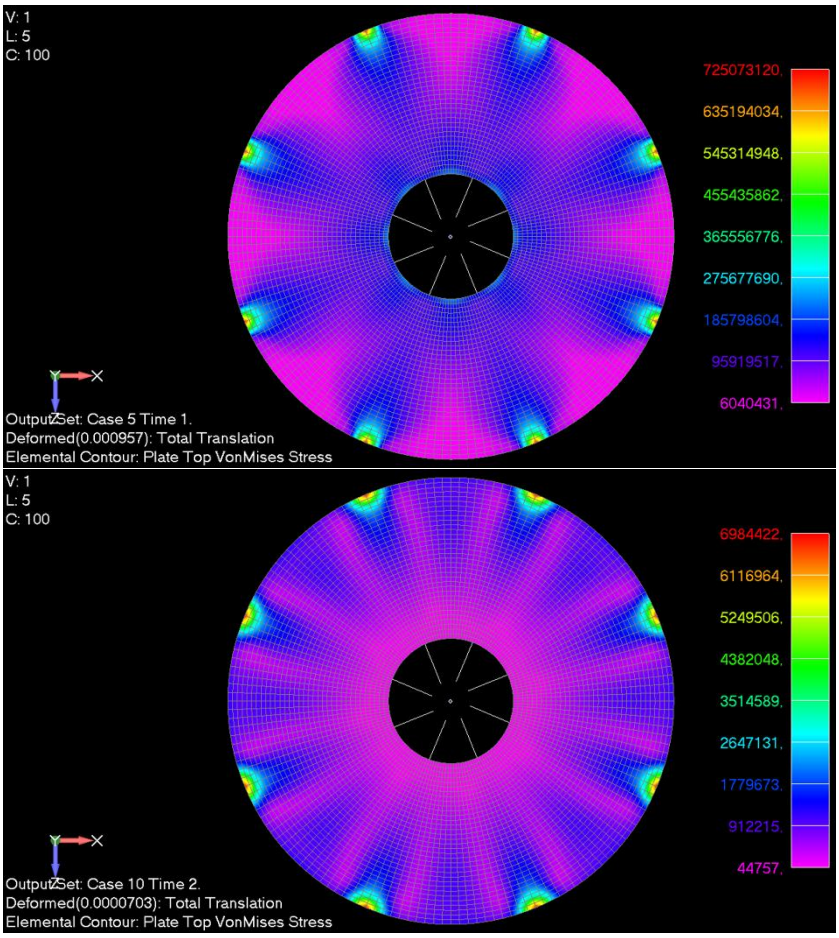

Fully stretched shield (end step 1)

Linked and recovered shield (end of step 2)

DOI: 10.13009/EUCASS2023-091

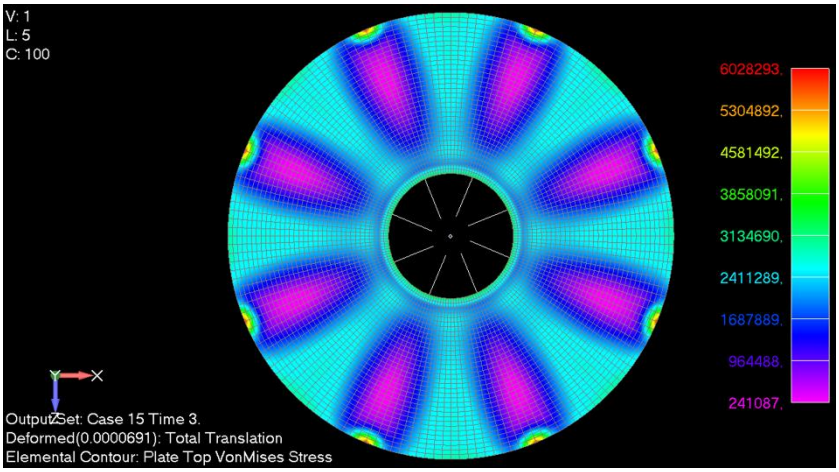

Shield under the action of the external loads (end of step 3)

Figure 13. Displacement and stress on the shield during the simulation steps, top view.

4.2 Flexible TPS and deployable mechanism

The deployment mechanism, consisting of ribs and struts, shall be able to deploy and preload the flexible TPS with a tension high enough to guarantee a deflection of the TPS compatible with the aerodynamic requirements. Such a preload shall be maintained by the actuation mechanism during the whole mission time and conditions. Also, the deployed TPS shall be able to withstand the flight loads while preserving the aerodynamic characteristics of the capsule.

A further FE model was then developed in Abaqus to account for both the flexible TPS and the inner deployment mechanism. The whole capsule is shown in Figure 14 while the TPS geometry and mesh are detailed in Figure 15. The rigid part of the heat shield, requiring high thermal performance to withstand the thermal loads at the nose of the capsule, is neglected at this stage of the project. The TPS is modelled by a pure membrane. Its properties were considered by assuming the Nextel fiber characteristics (ultimate stress and elastic modulus) reported in the technical documentation [17]. However, further studies are being executed on a high-performance polybenzimidazole (PBI)-based thermoplastic material to investigate its capability to efficiently dissipate the incident heat flux.

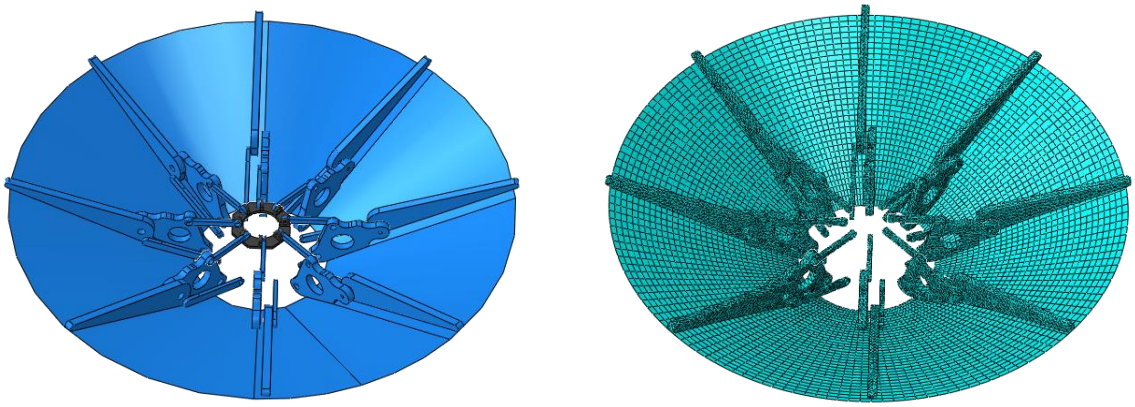

Figure 14. SPLASH capsule finite element model.

DOI: 10.13009/EUCASS2023-091

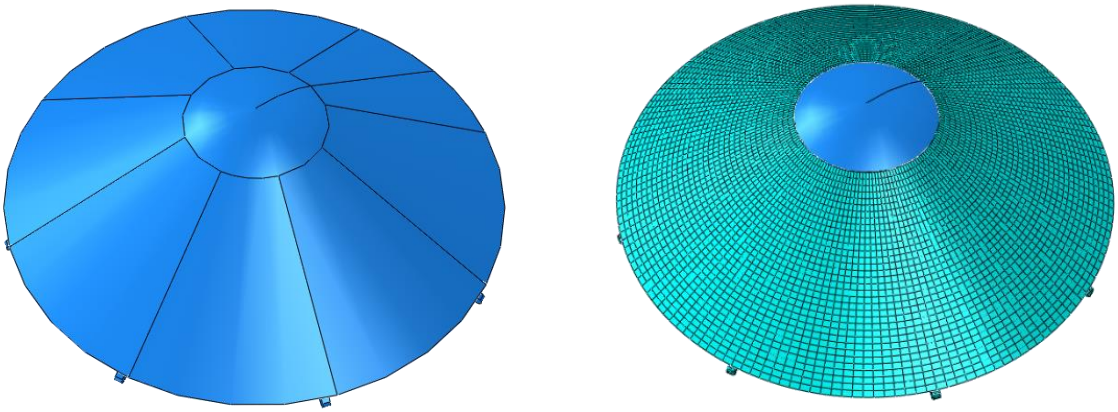

Figure 15. TPS geometry and mesh.

The load case was the preload of the membrane when the mechanism is deployed. The edges of the flexible TPS were connected to the ribs tips by means of rigid elements. Figure 16 and Figure 17 show the displacement and stress map in the flexible TPS induced by the preload. A maximum displacement of about 6.1 mm is obtained at the centre of the TPS membrane between the two points of connection with the inner mechanism. Furthermore, the stress distribution showed a maximum stress of 6.7 MPa.

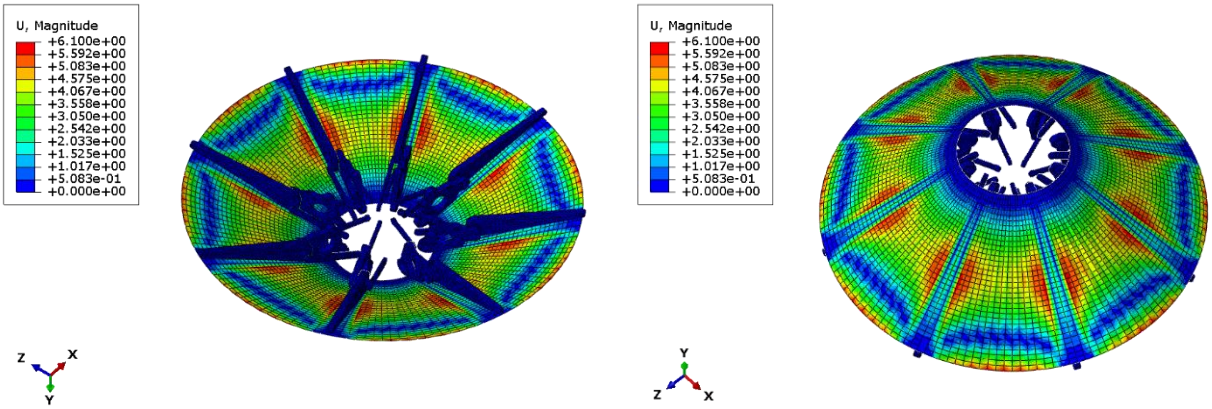

Figure 16. Displacement map in the flexible TPS induced by the preload

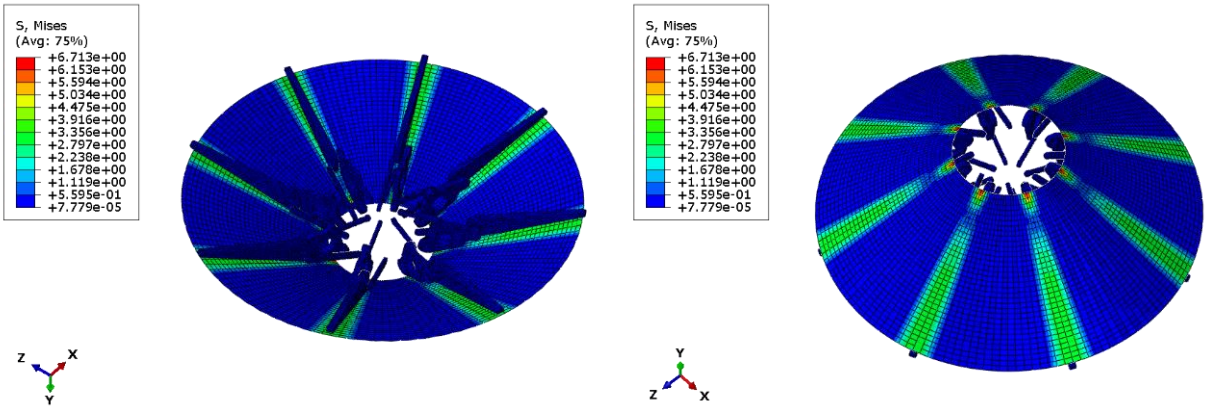

Figure 17. Stress map in the flexible TPS induced by the preload

5. Conclusions

A critical requirement for mechanically deployable aeroshells design is an understanding of the factors influencing the structural interaction of the flexible thermal protection system and the amount of pre-tension that shall be put in the flexible heat shield by the deployable mechanism prior to atmospheric entry. Key design parameters such as the aerothermal heating and aerodynamic forces imparted on the vehicle may be significantly sensitive to the static

DOI: 10.13009/EUCASS2023-091

deflection imparted in the flexible heat shield by the entry flow field. Also, varying pre-tension in the heat shield may impact on the morphing ability of the aerosurface to correct re-entry trajectories through asymmetric shapes. The aeroelastic behaviour of the capsule may be also influenced by pre-tension and dynamic pressure.
In this paper, a dedicated study was conducted to improve structural modeling tools used in the design of SPLASH deployable morphing aeroshell for 12U CubeSat atmospheric re-entry. The activities included the definition of a reference mission with focus on trajectory analysis, aerothermal loads and dynamic pressure. A specific routine was developed to predict stress map in the flexible heat shield due to pre-tension as well as the related response due to the sizing pressure symmetrically distributed on the pretensioned shield. Deciding the appropriate pre-tension for a given mission requires a mission-specific trade study. After that, further simulations were carried out on the TPS membrane connected to the deployable mechanism. The model was representative of the most critical parts of the entire assembly in order to evaluate displacement and stress distribution of the structural components. As a next step, further simulations will be carried out by considering the peak dynamic pressure as well as the deceleration expected during the flight. Finally, the effect of creating an asymmetric shape by activating the SMA-based actuators embedded in the outer segments of the ribs will be investigated for missions requiring precision landing and/or aerocapture. This will require also a robust closed-loop guidance and control algorithm that can make on-the-fly adjustments to correct the trajectory by means of the envisaged smart actuation.

References

[1] D. Akin, “Applications of ultra-low ballistic coefficient entry vehicles to existing and future space missions”, in SpaceOps 2010 Conference Delivering on the Dream Hosted by NASA Marshall Space Flight Center and Organized by AIAA, 2010, p. 1928.

[2] Hughes, S.; Bailet, G.; Miller, N.; Korzun, A.; Zumwalt, C.; Cheatwood, F., Low Cost Innovative Atmospheric Entry Probes Combining CubeSat and HIAD Technologies” International Planetary Probe Workshop-13, 2016.

[3] Savino, R., Aurigemma, R., Aversana, P. D., Gramiccia, L., Longo, J., Maraffa, L., Punzo, F., and Scolamiero, L., “European Sounding Rocket Experiment on Hypersonic Deployable Re-Entry Demonstrator Background of the Project,” 8th European Symposium on Aerothermodynamics for Space Vehicles, 2015.

[4] Cassell, A., Smith B. P., Wercinski P. F., Ghassemieh S. M., Hibbard K.E., Nelessen A. P., and Cutts J. A., ADEPT, A Mechanically Deployable Re-Entry Vehicle System, Enabling Interplanetary CubeSat and Small Satellite Missions, SSC18-XII-08, 32nd Annual AIAA/USU Conference on Small Satellites.

[5] Danielle O' Driscoll, Paul J. Bruce and Matthew J. Santer. "Origami-based TPS Folding Concept for Deployable Mars Entry Vehicles," AIAA 2020-1897. AIAA Scitech 2020 Forum. January 2020.

[6] Justin S. Green, Barry Dunn and Robert Lindberg. "Morphing Hypersonic Inflatable Aerodynamic Decelerator" AIAA 2013-1256. AIAA Aerodynamic Decelerator Systems (ADS) Conference. March 2013.

[7] Fedele, A., Omar, S., Cantoni, S., Savino, R., & Bevilacqua, R. 2021, Precise re-entry and landing of propellantless spacecraft, Advances in Space Research, 68 (2021), 4336-4358, doi: 10.1016/j.asr.2021.09.029

[8] R. Savino, V. Carandente, Aerothermodynamic and feasibility study of a deployable aerobraking re-entry capsule, Fluid Dynamics and Material Processing 8(4) pp. 453-477 (2012).

[9] Fedele, A. (2020). A deployable aerobraking system for atmospheric reentry. In PhD thesis in Industrial Engineering. http://dx.doi.org/10.13140/RG.2.2.34074.36801.

[10] Vanhamel , J., Eaton, N., & Spreij, R. (2022). using fiber bragg gratings for shape monitoring and adjustment of a thermal protection system aboard a targeted re-entry cubesat. Paper presented at The 2nd International Conference on Flight Vehicles, Aerothermodynamics and Re-entry Missions Engineering (FAR), Heilbronn, Germany.

[11] Reddish, B.J., Nikaido, B.E., D'souza, S.N., Hawke, V.M., Hays, Z.B., & Kang, H.S. (2020). Pterodactyl: Aerodynamic and Aerothermal Modeling for a Symmetric Deployable Earth Entry Vehicle with Flaps, AIAA 2021-0763. AIAA Scitech 2021 Forum. January 2021.

[12] D’souza S.N., Alunni A., Yount B., Okolo W., Margolis B., Johnson B.J., Hibbard K., Barton J., Hawke V.M., Hays Z.B., Reddish B. and Rocca-Bejar D., Pterodactyl: System Analysis of an Asymmetric and Symmetric Deployable Entry Vehicle for Precision Targeting Using Flaps, AIAA 2021-0762. AIAA Scitech 2021 Forum. January 2021.

[13] Dimino, I.; Vendittozzi, C.; Reis Silva, W.; Ameduri, S.; Concilio, A. A Morphing Deployable Mechanism for Re-Entry Capsule Aeroshell. Appl. Sci. 2023, 13, 2783. https://doi.org/10.3390/app13052783.

[14] B. Smith, A. Cassell, C. Kruger, E. Venkatapathy, C. Kazemba and K. Simonis, "Nano-ADEPT: An entry system for secondary payloads," 2015 IEEE Aerospace Conference, Big Sky, MT, USA, 2015, pp. 1-11, doi: 10.1109/AERO.2015.7119095.

[15] Paolo Scaramuzzino (2023). Hypersms Aerothermodynamics tool (https://www.mathworks.com/matlabcentral/fileexchange/54103-hypersms-aerothermodynamics-tool), MATLAB Central File Exchange. Retrieved July 8, 2023.

DOI: 10.13009/EUCASS2023-091

[16] P Vernillo, A Fedele, R Gardi, R Savino, F Punzo, F Gunnar, and R Molina, “Mini-irene: The first european flight experiment of a deployable heat shield”, in 23rd ESA Symposium on European Rocket and Balloon Programmes and Related Research, 2017.
[17] https://thermostatic.com/nextel/files/notebook.pdf, 3M Nextel, Ceramic Textiles Technical Notebook.

Acknowledgments

This research is funded in part by a grant from the Italian Ministry of Foreign Affairs and International Cooperation (MAECI) for the Italian side, and by a grant from the National Council of State Research Support Foundations (CONFAP), through the involved State Distrito federal Funding Agencies (FAPDF) for the Brazilian side, in the framework of the first Executive Programme for Scientific and Technological Cooperation between the Government of the Italian Republic and the Government of the federal Republic of Brazil.